



Synthesis, Ion-exchange, Structural Characterization and Adsorption of K, Na-FER Type Zeolite

YINGCAI LONG*, MINGHUA MA¹, YAOJUN SUN² and HUIWEN JIANG¹

¹Department of Chemistry, Fudan University, Shanghai 200433, P.R. China

²Center of Analysis and Measurement, Fudan University, Shanghai 200433, P. R. China

(Received: 27 January 1999; in final form: 16 September 1999)

Abstract. Synthesis of K, Na -FER type zeolite was studied in the reactant system of K_2O — Na_2O — Al_2O_3 — SiO_2 — CO_3 — HCO_3 — H_2O . Sodium silicate, silica sol and fumed silica were tested as the silica source, and solid aluminum sulfate, aluminum hydroxide and meta-kaolinite as the alumina source. The starting materials, the composition of the reactant, and the synthesis temperature greatly influence the phases crystallized. A pure phase of K, Na-FER zeolite was hydrothermally prepared at 208 °C with sodium silicate and solid aluminum sulfate as starting materials. The optimum composition of the reactant for synthesis of the pure FER zeolite was determined. Chemical analysis, XRD, FT-IR, ²⁹Si and ²⁷Al MAS NMR, TG/DTA, and adsorption of nitrogen, methanol and *n*-hexane were used to characterize the zeolite and compared with the reference sample of perfect single crystals of siliceous FER zeolite. The content of K^+ and Na^+ in the zeolite decreases gradually with the times of the treatment of ion-exchange/calcination, leading to an increase in the adsorption capacities of nitrogen and methanol, and a decrease of the loading of *n*-hexane. The location of the K^+ , the stacking faults, and dealumination of the zeolite framework are discussed based on the ion exchange and adsorption behavior.

Key words: FER type zeolite, synthesis, ion exchange, structural characterization, sorption

1. Introduction

FER type zeolite (Ferrierite) is an aluminosilicate molecular sieve with 10-ring medium pore openings. The secondary building unit of the FER framework is 5-ring, which is similar to that of MFI (ZSM-5) Zeolite. FER zeolite was first found as a mineral in nature. There are several isotopic structures of the FER framework named as ZSM-35, FU-9, NU-23 etc. synthesized in different reactant systems. The crystal system of FER is orthorhombic with a space group of Immm [1]. The catalytic properties of the zeolite for hydrocarbon cracking is remarkable. In recent years, the zeolite has been found to exhibit an excellent shape-selectivity in the catalysis of isomerization of *n*-butene to iso-butene. Iso-butene is a raw material for producing MTBE (methyl *tert*-butyl ether), an additive in lead-free gasoline.

* Author for correspondence. Tel: (+86)-21-6564-3913; FAX: (+86)-21-6564-1740; E-mail address: yclong@fudan.edu.cn.

Therefore, more attention has been paid to the zeolite for its role in environmental protection [2].

FER type zeolite can be prepared in the reactant with or without an organic template. Coombs et al. synthesized FER zeolite at 330 °C using Na and Ca alumino-silicate as raw materials [3]. Senderov [4] obtained a co-crystallite of FER with mordenite, and Sand [5] prepared a co-crystallite of FER with quartz and analcime respectively in the reactant of Na- alumino-silicate at high temperature. Sr-containing FER zeolite was prepared by Barrer and Marshall [6] and Hawkins [7] at 340 °C for 10 days. Winquist prepared FER zeolite at 175–210 °C using silica-alumina gel with Na_3PO_4 and KF [8]. Na, K-FER zeolite was synthesized at above 256 °C in the reactant system of silica-alumina gel and Na and K carbonate with stirring [9]. In order to reduce contamination and lower the cost of production, it is useful to investigate the synthesis of the zeolite using cheaper starting materials and at mild conditions.

The ratio of silica/alumina in FER zeolites varies with the composition of the reactant. This leads to a remarkable variety of structural properties. Some works related to the crystal structure [10–14], and adsorptive properties [14–17] of FER type zeolite were reported. No investigation was published on the structural, ion exchange and adsorption of FER zeolite synthesized in the $\text{K}_2\text{O}-\text{Na}_2\text{O}-\text{Al}_2\text{O}_3-\text{SiO}_2-\text{CO}_3-\text{HCO}_3-\text{H}_2\text{O}$ system.

In this paper, we report the successful synthesis of pure K, Na-FER zeolite in the reactant of $\text{K}_2\text{O}-\text{Na}_2\text{O}-\text{Al}_2\text{O}_3-\text{SiO}_2-\text{CO}_3-\text{HCO}_3-\text{H}_2\text{O}$ at 208 °C. The major starting raw material used was water glass (an aqueous solution of sodium silicate), solid aluminum sulfate, K_2CO_3 and KHCO_3 . The structural property, the ion exchange in acid solution, and the adsorption behavior of the zeolite are investigated and compared with that of the single crystals of siliceous FER zeolite.

2. Experimental

2.1. SYNTHESIS

2.1.1. Chemicals

Silica and alumina sources: water glass (solution of sodium silicate, $\text{SiO}_2 = 28.15$ wt%, $\text{Na}_2\text{O} = 8.71$ wt%, $\text{H}_2\text{O} = 63.14$ wt%); silica sol ($\text{SiO}_2 = 27.06$ wt%, $\text{Na}_2\text{O} = 0.152$ wt%, $\text{H}_2\text{O} = 72.79$ wt%); fumed silica (an amorphous silica, $\text{SiO}_2 = 98.0$ wt%, $\text{H}_2\text{O} = 2.0$ wt%); meta-kaolinite ($\text{SiO}_2 = 45.08$ wt%, $\text{Al}_2\text{O}_3 = 38.26$ wt%, $\text{Fe}_2\text{O}_3 = 0.56$ wt%); solid reagent with analytically pure: $\text{Al}_2(\text{SO}_4)_3$ and $\text{Al}(\text{OH})_3$.

Other analytically pure reagents: solid reagent of K_2CO_3 , KHCO_3 and NaOH ; H_2SO_4 (98 wt%); HF, *n*-propylamine and pyridine.

2.1.2. Synthesis Procedure

The source of silica (such as water glass, silica sol. etc.) was mixed with the source of alumina (such as solid $\text{Al}_2(\text{SO}_4)_3$ or $\text{Al}(\text{OH})_3$ etc.), then mixed with H_2SO_4 or

Table I. The influence of silica sources on the phases crystallized*

Silica Source	Period of reaction (h)						
	35	46	51	56	66	70	77
Water Glass	D	E	E	E	F	F	F
Silica Sol	D	E	E	E	F	F	F
Fumed Silica	D	E	E	E	E	E	E

* D, amorphous; E, co-crystallite of quartz and feldspar, F, co-crystallite of FER zeolite with quartz and feldspar.

NaOH to form a mixture. H_2SO_4 or NaOH were used to adjust the basicity of the reactant. Carbonate (such as solid K_2CO_3 and $KHCO_3$) and water were added to the mixture with vigorous stirring to form a homogeneous gel of the reactant. The gel was sealed in a 30 mL stainless steel autoclave, then hydrothermally crystallized in an oven at an established temperature in the range of 180–250 °C for 5–80 h under static conditions. The product was washed with distilled water, filtered, and then dried.

2.1.3. Influence of Silica Source and the Ratio of Na_2O/K_2O

The reactant was prepared with the molar composition of $(4.21Na_2O + 3.20K_2O) : Al_2O_3 : 13.5SiO_2 : 0.80CO_3 : 4.8HCO_3 : 4.01SO_4 : 130H_2O$ using solid $Al(OH)_3$ as the source of alumina. The reactant was hydrothermally crystallized at 250 °C for 35–77 h. Water glass, silica sol. and fumed silica were respectively used as the source of silica in the reactant for comparison. The as-synthesized products identified with XRD are listed in Table I. The result indicates that FER zeolite can be prepared in the reactant with both water glass and silica sol. as the source of silica. Water glass was used as the source of silica in the following synthesis tests because of its low cost. As investigated in Section 2.1.6, the reactant with lower water content is an advantage to the crystallization of FER zeolite. In this situation, the molar content of water can be lowered to 116 from 130 for further investigation using water glass as the silica source.

It was found that decreasing the ratio of Na_2O/K_2O to $4.21/6.55 = 0.64$ from $4.21/3.21 = 1.32$ obviously increased the crystallization rate of FER zeolite. Therefore, the period of the crystallization was kept in the range of 30–70 h while the temperature of the reaction was lowered to 220 °C. Since the source of K_2O is K_2CO_3 and $KHCO_3$, increasing the content of K_2O was accompanied by an increase of the content of CO_3 and HCO_3 in the reactant.

2.1.4. Influence of alumina source

The reactant was prepared with a molar composition of $(4.21Na_2O + 6.55K_2O) : Al_2O_3 : 13.5SiO_2 : 3.3CO_3 : 6.5HCO_3 : 5.96SO_4 : 116H_2O$, and hydrothermally

Table II. The influence of alumina sources on the phases crystallized*

Alumina source	Period of reaction (h)						
	26	30	35	46	51	61	70
Al ₂ (SO ₄) ₃	D	G	G	G	H	H	H
Al(OH) ₃	D	E	E	F	F	F	F
Meta-kaolinite	D	E	E	E	E	E	E

* The meaning of D, E and F is the same as that in Table I. G, co-crystallite of FER zeolite with quartz; H, co-crystallite of FER zeolite with quartz and tridymite.

reacted at 220 °C for 26–70 h. Solid Al₂(SO₄)₃, Al(OH)₃, meta-kaolinite were respectively used as the source of alumina in the synthesis for comparison. The as-synthesized products are listed in Table II. FER zeolite was synthesized in the reactant with both solid Al₂(SO₄)₃ and Al(OH)₃ as the source of alumina. Solid Al₂(SO₄)₃ was used as the source of alumina in the following synthesis tests because that chemical composition is more stable than that of Al(OH)₃ in air.

2.1.5. Influence of Reaction Temperature

The reactant was prepared with the molar composition the same as that in Section 2.1.4, and hydrothermally crystallized at the temperature of 250 °C, 220 °C, 208 °C and 180 °C for 26–70 h, respectively. The as-synthesized products are listed in Table III. FER zeolite with a small amount of quartz (<5%) formed in 26 to 30 h at a temperature of >220 °C, and then transformed to a co-crystallite with tridymite. Lowering the reaction temperature to 208 °C, FER zeolite with a small amount of quartz crystallized in about 35 h, and remained without the formation of tridymite up to 70 h. The following synthesis tests were carried out at 208 °C.

Table III. The influence of reaction temperature on the phases crystallized*

Reaction temp. (°C)	Period of reaction (h)						
	26	30	35	46	51	61	70
250	G	G	H	H	H	H	H
220	D	G	G	G	H	H	H
208	D	D	G	G	G	G	G
180	D	D	D	D	D	D	D

* The meaning of D, G and H is the same as that in the table above.

Table IV. The influence of water content on the phases crystallized*

<i>m</i> (water content)	Period of reaction (h)				
	34	37	41	46	58
215.8	D	D	D	D	D
130.4	D	D	D	D	G
115.7	G	G	G	G	G

* The meaning of D and G is the same as that in the table above.

2.1.6. Influence of Water Content

The reactant was prepared with the molar composition of $(4.21\text{Na}_2\text{O} + 6.55\text{K}_2\text{O}) : \text{Al}_2\text{O}_3 : 13.5\text{SiO}_2 : 3.3\text{CO}_3 : 6.5\text{HCO}_3 : 5.96\text{SO}_4 : \mathbf{m}\text{H}_2\text{O}$. The reaction was carried out at 208 °C for 34–58 h. The as-synthesized products are listed in Table IV. It seems that the lower the content of water in the reactant, the shorter the period for crystallization of FER zeolite. FER zeolite with a little impurity of quartz (<1%) formed at 58 h and 34 h respectively for $\mathbf{m} = 130.4$ and 115.7 in the reactant. On the other hand, the reactant remained amorphous up to 58 h when $\mathbf{m} = 215.8$. Since the content of water in water glass used in this study was about 63 wt%, the lowest \mathbf{m} in the reactant was restricted to 115.7.

2.1.7. Influence of Basicity

The molar composition of the reactant was $(4.21\text{Na}_2\text{O} + 6.55\text{K}_2\text{O}) : \text{Al}_2\text{O}_3 : 13.5\text{SiO}_2 : 3.3\text{CO}_3 : 6.5\text{HCO}_3 : \mathbf{x}\text{SO}_4 : \mathbf{y}\text{NaOH} : 116\text{H}_2\text{O}$. H_2SO_4 or NaOH was used to change \mathbf{x} or \mathbf{y} in the reactant, respectively. The synthesis was carried out at 208 °C in the reaction period of 6–52 h. Table V lists the as-synthesized phases. Pure FER zeolite appeared at 9 h when $\mathbf{x} = 4.26$ and $\mathbf{y} = 0$. On the other hand, the zeolite formed in the reactant at 33 h while increasing \mathbf{x} to 6.96. Therefore, the pure phase of K, Na-FER zeolite can be prepared in the reactants with the molar composition range of $\mathbf{x} = 3.0\text{--}7.0$ and $\mathbf{y} = 0\text{--}0.88$. The optimum range is $\mathbf{x} = 3.0\text{--}4.7$ and $\mathbf{y} = 0\text{--}0.1$. The zeolite with highest crystallinity was prepared in the reactant with $\mathbf{x} = 4.26$ and $\mathbf{y} = 0$. A kinetic curve of crystallization was measured in the reactant with the optimum composition at 208 °C. The sample of pure FER zeolite, prepared in the reactant described in the next section, was used as the reference for measuring the kinetic curve. The curve indicates that the pure phase of FER zeolite with the relative crystallinity >95% is obtained in the reaction period of 22–35 h at 208 °C.

Table V. The influence of basicity on the phases crystallized*

Reaction period (h)	x	Reactant composition (4.21Na ₂ O+6.55K ₂ O) : Al ₂ O ₃ : 13.5SiO ₂ : xSO ₄ : yNaOH: 3.3CO ₃ : 6.5HCO ₃ : 115.7H ₂ O					
		6.96	4.56	4.26	3.0	3.0	3.0
	y	0	0	0	0	0.48	0.88
6		D	D	D	D	D	D
9		D	D	I	I	I	I
12		D	D	I	I	I	I
15		D	D	I	I	I	I
18		D	I	I	I	I	I
21		D	I	I	I	I	I
24		D	I	I	I	G	G
27		D	I	I	I	G	G
30		D	I	I	I	G	G
33		I	G	G	G	G	G
36		I	G	G	G	G	G
40		G	G	G	G	G	G
44		G	G	G	G	G	G
48		G	G	G	G	G	G
52		H	G	G	G	H	H

* The meaning of D, G and H is the same as that in the table above; I-denotes the pure phase of FER zeolite.

2.1.8. Preparation of Samples for Characterization

K, Na-FER zeolite was prepared with water glass, solid aluminum sulfate, solid K₂CO₃ and KHCO₃, H₂SO₄, and distilled water as starting materials. The molar composition of the reactant was (4.21Na₂O+6.86K₂O) : Al₂O₃ : 13.5SiO₂ : 3.62CO₃ : 6.52HCO₃ : 3.27SO₄ : 116H₂O. The procedure for preparing the reactant was different from that stated in Section 2.1.2, because of the larger scale of the synthesis. The solid mixture composed of 23.38 g K₂CO₃ and 33.84 g KHCO₃ was ground, then mixed with 150 g water glass to form a uniform mixture (I) after vigorous stirring. 17.76 g of solid Al₂(SO₄)₃ was mixed with 13.6 g distilled water and 21.03 g H₂SO₄ to get a mixture (II). Mixture (II) was added to mixture (I) to form a homogeneous gel of the reactant with vigorous stirring in a domestic food processor. The reactant was hydrothermally treated at 208 °C for 27–45 h in a 400 mL autoclave under static conditions. After washing, filtering and drying, the as-synthesized K, Na-FER zeolite (Sample A) was ion-exchanged with 1 N HCl solution with 1/10 of solid/liquid ratio at 100 °C for 5 h, then calcined at 550 °C for 16 h to yield Sample B1. Sample B1 was treated under the same conditions described above, and then calcined at 550 °C for 5 h, yielding Sample B2.

Samples B3 and B4 were prepared from Sample B2 using the same procedure of ion-exchange/calcination once and twice, respectively.

The single crystals of siliceous FER zeolite used as the reference sample were synthesized according to the literature [11]. The starting materials used in the synthesis were: fumed silica, *n*-propylamine, pyridine, HF/Py (a solution of HF with 70 wt% of pyridine) and distilled water. The molar ratio of the reactant was: 16.0 pyridine : 1.5SiO₂ : 8.0H₂O : 4.0 *n*-propylamine : 2.0HF/Py. Pyridine and *n*-propylamine were mixed with water to get a solution (I). The solution of HF/Py and fumed silica were added to solution (I) under vigorous stirring to yield a uniform gel of the reactant. The gel was sealed in a 30 mL stainless steel autoclave lined with Teflon, and heated to 220 °C for 6–7 d. The as-synthesized product was filtered, washed with distilled water and dried, and then calcined at 850 °C for 16 h to remove the organic template, giving the reference sample (Sample C).

2.2. CHARACTERIZATION

The shape and the size of the zeolite crystallites were observed using polarization microscopy and a TSM-1 scanning electron microscopy. The SiO₂ and Al₂O₃ contents of the zeolite samples were chemically analyzed. The Na₂O and K₂O content were measured with an atomic absorption spectrometer. The content of Al₂O₃ in Sample C was determined using inductively coupled plasma (ICP) with a Jarrell-Ash Division Atomscan 2000 ICP spectrometer.

X-ray powder diffraction (XRD) of the zeolite samples was carried out using a Rigaku D-MAX/II A X-ray powder diffractometer with Cu K α radiation in the 2θ range of 5–35 ° at a scanning speed of 16°/min. FT-IR spectra were obtained with a Nicolet Magna-500 IR spectrometer in a scanning range of 400–2000 cm⁻¹ using KBr pellets. TG/DTA measurements were carried out by using a Rigaku PTC-10A thermal analyzer with airflow of 70 mL/min at a rate of 5 °C/min from room temperature to 1300 °C. About 10–20 mg of the zeolite sample was used for each test.

The ²⁹Si and ²⁷Al magic-angle spinning nuclear magnetic resonance (MAS NMR) spectra of the samples were recorded at room temperature using a Bruker MSL-300 spectrometer. The ²⁷Al resonance frequency used was 78.205 MHz, and the rotor was spun at 3.5 KHz. The rf field was 27.8 KHz, corresponding to a $\pi/2$ pulse width of 5.5 ms; recycle time = 500 ms. AlCl₃(H₂O)₆ was used as a reference. The ²⁹Si resonance frequency used was 59.595 MHz, and the rotor was spun at 4.0 KHz. The rf field was 37.0 KHz, corresponding to a $\pi/3$ pulse width of 4.5 ms; recycle time was 2 s; Q₈M₈ was used as a second reference for the ²⁹Si chemical shift. The numbers of NMR scans (NS) were 600–3000.

The adsorption isotherms of methanol and *n*-hexane were measured at 30 ± 0.1 °C with a Sartorius-7012 vacuum super-micro electron-balance. Before measurement about 100 mg of zeolite sample was dehydrated at 350 °C for 1 h in vacuum of the balance. Methanol and *n*-hexane used as the adsorbate were analytically

Table VI. Chemical composition of FER zeolite samples

Sample	Content (wt%)					SiO ₂ /Al ₂ O ₃ (in mole)
	SiO ₂	Al ₂ O ₃	Na ₂ O	K ₂ O	H ₂ O	
A	86.16	5.68	1.07	3.63	3.44	25.8
B1	89.49	5.69	0.080	3.70	1.05	26.7
B2	89.53	5.67	0.040	1.99	2.77	26.8
B3	89.61	5.67	0.0064	0.089	4.63	26.8
B4	90.02	5.52	<0.0064	0.031	4.36	27.7
C	99.51	0.080			0.41	1232

pure (content >99.99 wt%). The microporous volumes were determined from the adsorption and desorption isotherm of nitrogen at 77.35 K by using a Micromeritric ASAP 2000 instrument.

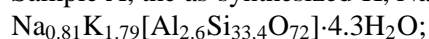
3. Results and Discussion

3.1. MORPHOLOGY AND CHEMICAL COMPOSITION

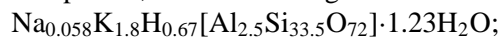
The crystallite of K, Na-FER zeolite is an agglomerate, 1 ~ 2 μm × 8 ~ 9 μm in size (see Figure 1a). The reference siliceous FER zeolite is a rhombic flake, perfect single crystals, 30 ~ 80 μm long (See Figure 1b).

The chemical compositions of the samples are listed in Table VI. The cell compositions are as follows:

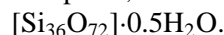
Sample A, the as-synthesized K, Na-FER zeolite,



Sample B1, the ion-exchanged FER zeolite,



Sample C, the calcined reference sample,



After one ion exchange treatment, the content of Na⁺ in Sample A decreases by 92%. Otherwise, the content of K⁺ is almost the same as that in the as-synthesized zeolite. After three treatments with ion-exchange/calcination, the content of K⁺ decreases to <0.1 wt%. This fact implies that the cations of K⁺ may locate in the small cages, the intersections of 8-ring channels with 6-ring channels, where it is difficult for the aqueous ion of H⁺ to enter for direct exchange with K⁺. The cations of K⁺ migrate into 10-ring channels in the case of calcination at higher temperature, leading to easier ion exchange.

The ²⁷Al MAS NMR spectrum indicates that there are framework Al (chemical shift at 55 ppm) and a trace of extra-framework Al (chemical shift at 0 ppm) [18] in the samples. The extra-framework Al is usually easily removed by acid



a



b

Figure 1. Morphology of as-synthesized samples. (a) K, Na-FER zeolite, $\times 1000$, (b) siliceous FER zeolite, $\times 70$.

treatment. In fact, the ratio of silica/alumina slightly increases with the treatment of ion-exchange/calcination for Sample A (see Table VI), indicating that the dealumination of the framework Al from FER zeolite is difficult by this method.

3.2. XRD PATTERNS

The position and the relative intensity of the diffraction peaks for FER zeolite samples (see Figure 2) are consistent with Reference [10]. The sum intensity of five strong peaks (at 9.5° , 22.6° , 23.8° , 24.2° , and $24.9^\circ/2\theta$) is 16.7 for Sample A, and 21.4 for Sample B1. It seems that the crystallinity of the sample increases

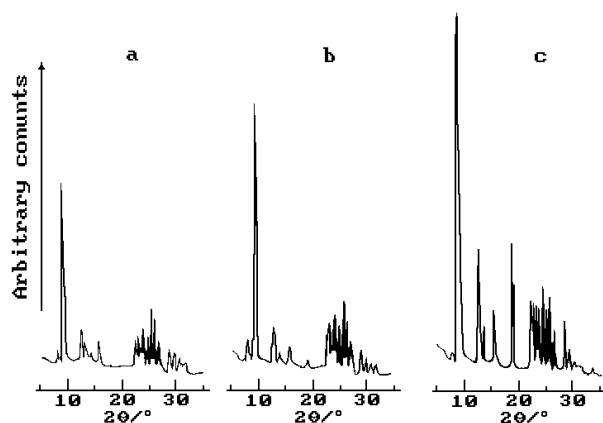


Figure 2. XRD patterns of samples. (a) as synthesized K, Na-FER zeolite (Sample A); (b) after treated once with ion-exchange/calcination (Sample B1); (c) as synthesized siliceous FER zeolite.

with acid treatment. This is because some soluble salt and amorphous species in Sample A were removed. The intensity of the peaks at 9.5° and $19^\circ/2\theta$ shown in the XRD pattern of siliceous FER zeolite is extremely high. The phenomenon is due to the optimum orientation of the single crystals of the zeolite on the XRD test plate. In this case the (200) and (400) reflection planes are parallel to the surface of the sample discs. It is reasonable to believe that the comparison of the crystallinity with the method above is not suitable in some cases.

3.3. FT-IR SPECTRA

FT-IR spectra of as-synthesized FER zeolite samples (see Figure 3A) are consistent with that of Reference [19]. In the spectrum of Sample A, the vibration peak at 1632 cm^{-1} belongs to the adsorbed water. The peak at 1219 cm^{-1} is assigned to an asymmetric stretch vibration in the tetrahedron. The peaks at 1079 cm^{-1} and 794 cm^{-1} can be assigned, respectively, to the vibration of the asymmetric and the symmetric stretch of the external linkages. The peaks at 591 cm^{-1} and 463 cm^{-1} , are caused by the vibrations of the double-ring and T-O bend in the framework, respectively. The resolution of the IR vibrations is obviously higher for the single crystals of siliceous FER zeolite. Some fine vibrations appear in the range of $1082\text{--}1235\text{ cm}^{-1}$ and $500\text{--}830\text{ cm}^{-1}$, indicating the perfect structure of the single crystals of siliceous FER zeolite. The lower resolution of Sample A may indicate that there are more defects of stacking faults in the structure. In general, the vibration of the asymmetric stretch at 1079 cm^{-1} shifts to higher frequency on increasing the ratio of silica/alumina in the zeolite framework. The vibration is at 1078 , 1082 , 1082 , and 1085 cm^{-1} respectively in the spectrum of Samples B1, B2, B3 and B4 (see Figure 3B), proving the progressive dealumination of the zeolite framework,

which was treated with ion-exchange/calcination for various times. The vibration shifts more for Sample B4 than that for Sample B2 and Sample B3. This may be caused by the greater dealumination in the framework of Sample B4.

3.4. TG/DTA

There were a few reports related to the thermal stability of FER zeolite [10]. The weight loss below 400 °C on the TG curve is attributed to the dehydration of the zeolite. The TG/DTA curves and the further identification with XRD proved that the framework of the as-synthesized K, Na-FER zeolite collapsed and transformed to cristobalite at a temperature of 1019 °C. The temperature of the phase transformation of Sample B1 rose to 1170 °C due to less Na⁺ in the zeolite, indicating an improvement of the thermal stability with the ion-exchange treatment in acid solution. This fact indicates the framework of FER zeolite possesses very high stability both on heating and on acid treatment. This is because its silica rich framework and 5-ring secondary unit, which is similar to that of MFI (ZSM-5) zeolite.

3.5. ²⁹Si MAS NMR SPECTRA

Figure 4 shows ²⁹Si MAS NMR spectra of FER zeolite samples. A broader resonance peak, which is an overlap of several peaks, appears in the spectra of Sample B1. In general, the chemical shifts of the ²⁹Si resonance peaks are related to the chemical environment as follows: -81 to -91 ppm for Si(4Al), -85 to -94 ppm for Si(3Al), -91 to -99 ppm for Si(2Al), -96 to -106 ppm for Si(1Al), and -101 to -115 ppm for Si(0Al) [20, 21]. Computer simulation with Gaussian fits of the NMR spectra shows six resonance peaks at -100.5 ppm, -103.3 ppm, -106.7 ppm, -109.4 ppm, -114.3 ppm, and -118.2 ppm for Sample B1 (see Figure 4c). It indicates that Si(1Al), Si(0Al) and silanol groups (at -103 ppm) exist in the sample [18]. There are five locations of the Si atom with different chemical environments per asymmetry unit in the cell of FER zeolite with orthorhombic symmetry. Among them, Si(1) has four multi-positions, and Si(2) to Si(5) have eight multi-positions [20]. Four high resolution peaks, shown in the spectrum of Sample C, are in the range of -110 to -120 ppm, corresponding to Si(0Al) signals. No peak appears in the range of -96 to -109 ppm, indicating the perfect framework of siliceous FER zeolite without Si(1Al) and Si-OH. The result is consistent with that of FT-IR. The peaks at -111.4, -110.9, and -116.1 ppm are respectively related to the position of Si(2), Si(4) and Si(5). The peak at -115.3 ppm is an overlap of Si(1) and Si(3) signals, which is consistent with the report of Reference [13]. The broad resonance in the range of -110 to -118 ppm, which is the major portion in the spectrum of Sample B1, is the overlap of Si(1) to Si(5) signals, corresponding to Si(0Al).

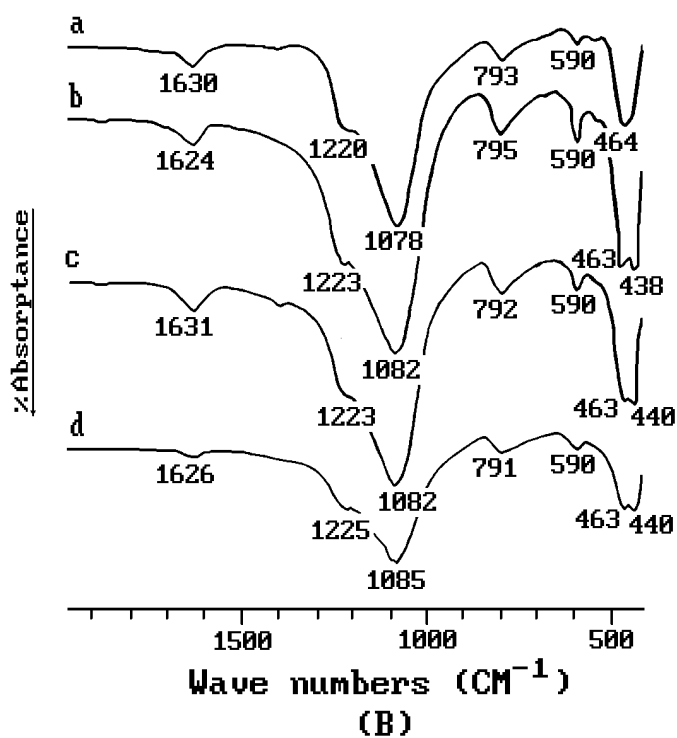
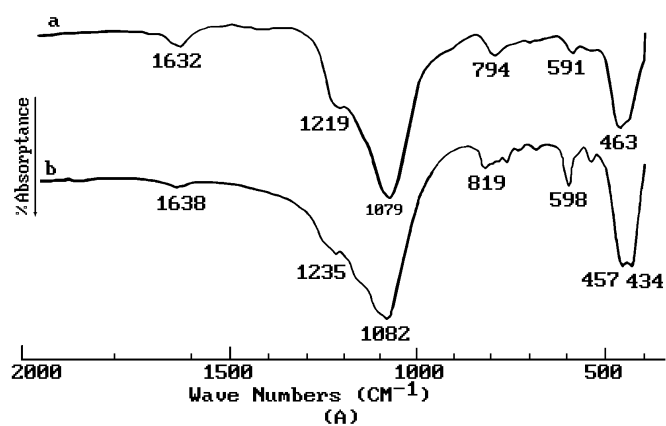


Figure 3. FT-IR spectra of A: as-synthesized K, Na-FER zeolite (a), and siliceous FER zeolite (b); B: K, Na-FER zeolite samples treated with ion-exchange/calcination (a) once (Sample B1); (b) twice (Sample B2); (c) three times (Sample B3); (d) four times (Sample B4).

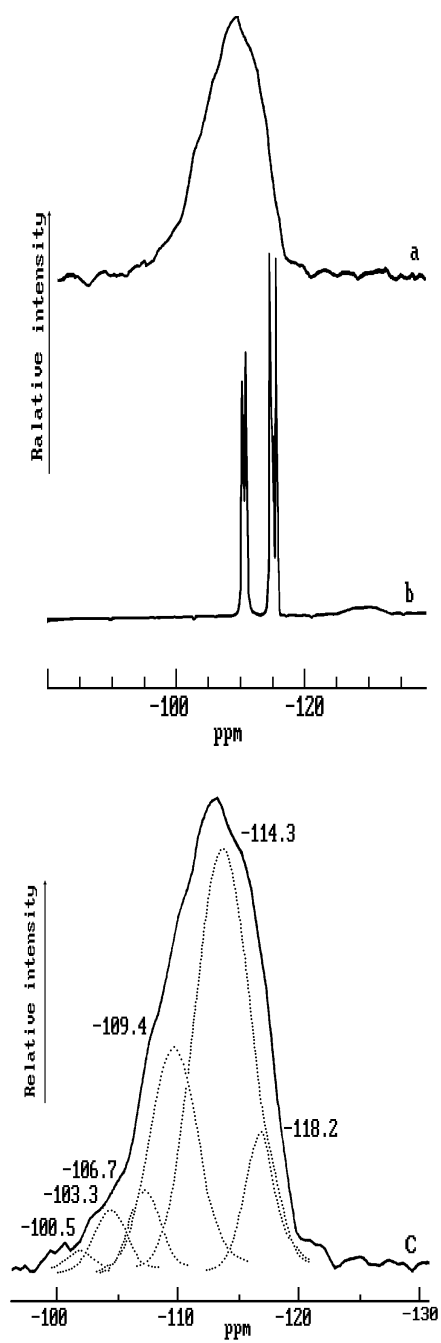


Figure 4. ^{29}Si MAS NMR spectra of (a) K, Na-FER zeolite after treated once with ion-exchange/calcination (Sample B1); (b) siliceous FER zeolite after calcination at 850 °C for 16 h (Sample C); (c) the spectrum of Sample B1 with Gaussian fits by computer.

Table VII. Microporous volume and adsorption capacity at $P/P_0 = 0.60$ on FER zeolite samples at 30 °C

Sample	Microporous volume* (cm ³ /g) (V_1)	Adsorption capacity (mL/g)			
		Methanol (V_2)	V_2/V_1	<i>n</i> -Hexane (V_3)	V_3/V_1
B1	0.115	0.072	0.63	0.064	0.56
B2	0.132	0.080	0.61	0.056	0.42
B3	0.136	0.085	0.63	0.055	0.40
B4	0.136	0.073	0.54	0.054	0.40
C	0.138	0.088	0.64	0.071	0.51

* The data of microporous volume are determined with the adsorption of nitrogen at 77K.

3.6. ADSORPTION

The adsorption isotherms of nitrogen (0.36 nm), methanol (0.43 × 0.56 nm) and *n*-hexane (0.43 × 1.03 nm) are Type I, the typical microporous adsorption on FER zeolite. Table VII summarizes the adsorption data.

In the cell of FER zeolite, two 10-ring channels with window size of 0.43 × 0.55 nm and a length of 0.749 nm are along the [001] direction. Two 6-ring channels are in that direction as well. On the other hand, two 8-ring channels with a pore opening of 0.34 × 0.48 nm and a length of 1.413 nm are parallel to [010]. A small cage with diameter of 0.6–0.7 nm locates at the intersection of the 8-ring channel with the 6-ring channel [22, 23]. Comparing the window size with the molecular size, it can be estimated that N₂ is adsorbed in both 8-ring and 10-ring channels, and methanol and *n*-hexane are only adsorbed in 10-ring channels. The microporous volume, determined with N₂ adsorption on Sample B3, is 98% of that on the single crystals of siliceous FER zeolite (Sample C), indicating the high crystallinity of H-FER zeolite prepared from the as-synthesized K, Na-FER zeolite. The significant decrease of the K⁺ content of Samples B2 and B3 obviously increases the microporous volume (see Table VII and Figure 5). This fact supports the deduction in Section 3.2, that the cations of K⁺ mainly locate in the small cages of the as-synthesized K, Na-FER zeolite.

In high silica zeolites, cations and silanol groups usually act as strong electrostatic centers of adsorption. The framework O²⁻, which covers the whole surface of the perfect siliceous zeolite, also act as adsorption centers. The adsorbed molecules react with the framework O²⁻ with van der Waals force. Therefore, the siliceous zeolite is usually hydrophobic and organophilic [24, 25].

The adsorption volume of methanol is obviously lower than that of *n*-hexane on the siliceous FER zeolite at $P/P_0 < 0.05$ (see Figure 5 and 6). On the other hand, the adsorption of methanol is evidently higher than that of *n*-hexane on Samples B1, B2 and B3 at low partial pressure. Chemical analysis and ²⁹Si MAS NMR have proved that cations and silanol groups are present in K, Na-FER zeolite and absent

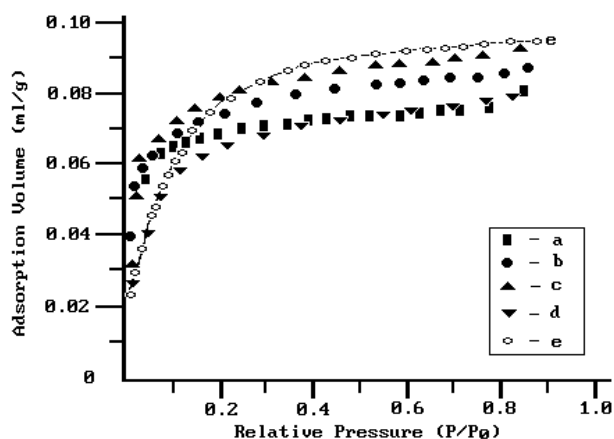


Figure 5. Methanol adsorption isotherms at 30 °C on K, Na-FER zeolite samples treated with ion-exchange/calcination (a) once (Sample B1); (b) twice (Sample B2); (c) three times (Sample B3); (d) four times (Sample B4); and (e) siliceous FER zeolite after calcination at 850 °C for 16 h (Sample C).

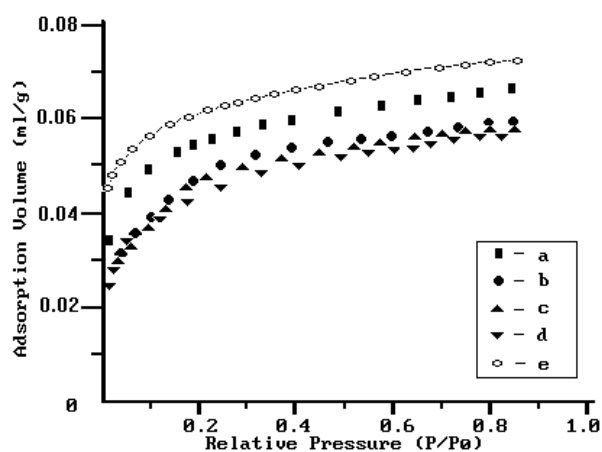


Figure 6. *n*-Hexane adsorption isotherms at 30 °C on K, Na-FER zeolite samples treated with ion-exchange/calcination (a) once (Sample B1); (b) twice (Sample B2); (c) three times (Sample B3); (d) four times (Sample B4); and (e) siliceous FER zeolite after calcination at 850 °C for 16 h (Sample C).

in siliceous FER zeolite. The H^+ , Na^+ and K^+ cations, and silanol groups act as the strong electrostatic centers of adsorption in the zeolite samples. The interaction of cations and silanol groups with the polar molecules of methanol is stronger than that with the non-polar molecules of *n*-hexane. On the contrary, siliceous FER zeolite exhibits weaker affinity with methanol and stronger affinity with *n*-hexane

because of the perfect framework, which is highly phobic to some polar molecules such as water etc.

Comparing the microporous volume (V_1) based on N_2 adsorption, and the adsorption volume of methanol (V_2) and n -hexane (V_3) (see Table VII), the following points can be suggested:

1. Siliceous FER zeolite possesses the maximum of V_1 , V_2 and V_3 , which is suitable for use as the standard.
2. The molecules of N_2 can enter 10-ring and 8-ring channel windows for occupying all of the micro-pores of the zeolite. Therefore, the adsorption volume of N_2 is the microporous volume. $V_3/V_1 = 0.51$ means about half of the microporous volume is available for n -hexane in siliceous FER zeolite. It is reasonable to believe that n -hexane is actually adsorbed in 10-ring channels. The deduction is consistent with the results by van Well *et al.* [15–17]. The cross-section of methanol molecules is the same as that of n -hexane. Differently, the molecule of methanol has a small end of —OH group. Part of the molecule is able to enter 8-ring channels, leading to $V_2/V_1 = 0.64$, which is obviously more than 0.51.
3. V_2/V_1 is in the range of 0.61–0.63 for Samples B1, B2 and B3. The data are very close to that for Sample C, indicating that methanol molecules enter part of the 8-ring channels of these samples as well.
4. V_1 , V_3 and V_3/V_1 is 0.115 CM^3/g , 0.064 ml/g and 0.56 respectively for Sample B1, in which the content of K_2O is 3.70 wt%. This fact also indicates that most of K^+ are located in the small cages of the sample, where N_2 is difficult to enter.

The phenomenon V_3 decreasing from Sample B1 to B4 (see Figure 6 and Table VII), is worth discussing. The molecular length of n -hexane is much longer than that of nitrogen and methanol and longer than the length of the 10-ring channel in the unit cell as well. After ion-exchange/calcination treatments of Samples B2 and B3, a small amount of K^+ migrates to the 10-ring channels from the small cages and disperses. The molecules of nitrogen and methanol may enter part of the small cages without K^+ , leading to an adsorption capacity increase. On the other hand, the small amount of K^+ , which dispersed in the 10-ring channels, restricts the adsorption of n -hexane and leads to a decrease of the loading. This fact implies that the stacking faults, which are present in the samples suggested in Section 3.3, may be perpendicular to the 10-ring channels in K, Na-FER zeolite, causing the channel loss straight in long range. Therefore, the stacking faults in the zeolite must influence the adsorption behavior of the adsorbed molecules of various sizes differently after treatment with ion-exchange/calcination. This is the reason why V_1 and V_2 increase, and V_3 decreases with the times of the treatment.

The contents of Na^+ and K^+ in Sample B4 are the lowest in all the samples of K, Na-FER zeolite investigated (see Table VI). But V_2 on Sample B4 is abnormally close to that on Sample B1 (see Table VII). The block of 10-ring channels and

8-ring channels with extra-framework Al might cause this phenomenon. Dealumination of the zeolite framework may be more serious when the content of Na⁺ and K⁺ in Sample B4 are extremely low, leading to the adsorption isotherm of methanol on Sample B4 close to that on siliceous FER zeolite at low partial pressure as well. This deduction is consistent with the result of FT-IR spectra.

4. Conclusions

1. The pure phase of K, Na-FER zeolite can be hydrothermally synthesized in the reactant of K₂O—Na₂O—Al₂O₃—SiO₂—CO₃—HCO₃—H₂O at 208 °C for 1–2 d in static condition. The source of silica and alumina used was the solution of sodium silicate and solid aluminum sulfate, respectively.
2. The K⁺ and Na⁺ cations were gradually removed from K, Na-FER zeolite, and H-FER zeolite was prepared with several treatments of ion-exchange/calcination.
3. Single crystal siliceous FER zeolite with a perfect framework is a good reference for investigating the structure and the adsorption of K, Na-FER samples.
4. The microporous volume and the loading of methanol increase, and the adsorption of *n*-hexane decreases with the removal of cations of K⁺ and Na⁺ from the zeolite samples. The adsorption behavior is related to the location of K⁺, the stacking faults, and the dealumination of the zeolite framework.

Acknowledgements

This work was supported by The Chinese National Natural Science Foundation (Grant CH29236120-03).

References

1. W. W. Meier, D. H. Olson, and Ch. Baerlocher: *Atlas of Zeolite Structure Types*, Fourth Revised Edition, Published on behalf of the Structure Commission of the International Zeolite Association, Elsevier, p. 106 (1996).
2. H. H. Mooiweer, K. P. Dejong, B. Kraushaar-Czarbetzki, W. H. J. Stork, and B. C. H. Krutzen: *Studies in Surface Science and Catalysis* **84C**, 2327 (1994).
3. D. S. Coombs, A. J. Ellis, W. S. Fyfe, and A. M. Taylor: *Geochim. Cosmochim. Acta.* **17**, 53 (1959).
4. E. E. Senderov: *Geokhimiya.* **9**, 820 (1959).
5. L. B. Sands: *First Int. Conf. Molecular Sieves* 71 (1967).
6. R. M. Barrer, and D. J. Marshall: *J. Chem. Soc.* 2296 (1964).
7. D. B. Hawkins: *Mater. Res. Bull.* **2**, 951 (1967).
8. B. H. C. Winqvist: *U.S. Patent* 3,933,974 (1976).
9. W. E. Cormier, and L. B. Sand: *U.S. Patent* 4,017,590 (1977).
10. H. Fjellvaag, K. P. Lillerud, and P. Norby: *Zeolites* **9**, 152 (1989).
11. R. E. Morris, S. J. Weigel, N. J. Henson, L. M. Bull, M. T. Janicke, B. F. Chmelka, and A. K. Cheetham: *J. Am. Chem. Soc.* **116**, 11849 (1994).

12. S. J. Weigel, J. Gabriel, E. G. Puebla, A. M. Bravo, N. J. Henson, L. M. Bull, and A. K. Cheetham: *J. Am. Chem. Soc.* **118**(10), 2427 (1996).
13. A. Davidson, S. J. Weigel, L. M. Bull, and A. K. Cheetham: *J. Phys. Chem. B.* **101**, 3065 (1997).
14. M. Ma, H. Jiang, Y. Long, and Y. Sun: *Acta Chimica Sinica.* **56**, 405 (1998).
15. W. J. M. van Well, X. Cottin, J. W. De Haan, R. A. Van Santen, and B. Smit: *Angew. Chem. Int. Ed. Engl.* **37**(8), 1081 (1998).
16. W. J. M. van Well, X. Cottin, B. Smit, J. H. C. Van Hooff, and R. A. Van Santen: *J. Phys. Chem. B.* **102**, 3952 (1998).
17. W. J. M. van Well, X. Cottin, J. W. De Haan, B. Smit, G. Nivarthi, J. A. Lercher, J. H. C. Hooff, and R. A. Van Santen: *J. Phys. Chem. B.* **102**, 3945 (1998).
18. Y. Long, M. Jin, Y. Sun, T. Wu, L. Wang, and L. Fei: *J. Chem. Soc., Faraday Trans.* **92**, 1647 (1996).
19. J. C. Jansen, F. J. van der Gssg, and H. Van Bekkum: *Zeolites* **4**, 369 (1984).
20. J. E. Lewis, Jr., C. C. Freyhardt and M. E. Davis: *J. Phys. Chem.* **100**, 5039 (1996).
21. J. Klinowski: *Ann. Rev. Mater. Sci.* **18**, 189 (1988).
22. C. L. Kibby, A. J. Perrotta, and F. E. Massoth: *J. Catalysis.* **35**, 256 (1974).
23. Y. Long, M. Zhu, Y. Sun, T. Wu, L. Wang, and L. Fei: *Chem. J. Chinese Univ.* **15**, 168 (1992) (in Chinese).
24. Y. Long, H. Jiang, and H. Zeng: *Langmuir* **13**, 4094 (1997).
25. H. Yang, Z. Ping, G. Niu, H. Jiang, and Y. Long: *Langmuir* **15**, 5382 (1999).